Dynamics of monatomic liquid metals

1991 J. Phys.: Condens. Matter 3 F53

(http://iopscience.iop.org/0953-8984/3/42/005)

J. Phys.: Condens. Matter 3 (1991) F53–F64. Printed in the UK

Dynamics of monatomic liquid metals

Wolfgang Gläser

Physik-Department, Technische Universität München, D-8046 Garching, Federal Republic of Germany

Received 20 May 1991, in final form 12 July 1991

Abstract. We shall summarize studies on the dynamics of monatomic liquids, mainly liquid metals, using inelastic neutron scattering techniques. Many microscopic properties of disordered systems like liquids which are not accessible by other techniques can be investigated by properly designed neutron scattering experiments. Details of the physics of diffusion processes, that is of single-particle motion, can be revealed by incoherent quasi-elastic scattering. Coherent scattering can explore relative motions or collective modes and their damping mechanism. Both aspects will be illustrated with a few examples of recent experiments.

1. Introduction

Although our general qualitative understanding of the liquid state of matter seems to be well developed the goal of eventually tracing the properties seen on macroscopic and microscopic scales back to the properties of the atomic constituents and the corresponding interatomic potentials is only slowly progressing.

An appropriate tool for the description of liquid properties on a microscopic scale is the pair correlation formalism. The static properties, the structures of liquids, can be revealed from structure factor measurements using x-ray and neutron diffraction techniques. As well as supplying complementary information to x-ray data on the structure neutrons can also offer the unique possibility of supplying detailed information on the atomic motions on the relevant time scale, that is on time-dependent correlation functions in the picosecond range.

Inelastic neutron scattering techniques have been essentially applied to the study of the dynamics of simple liquids like rare gas liquids and liquid metals. Liquid metals are interesting model systems because of their large liquid range.

Due to the lack of sufficient intensity and the need for suitable experimental techniques to determine absolute scattering cross sections it was only during the last two decades that sufficiently accurate measurements could be performed. It is the purpose of this article to summarize some more recent experiments on the dynamics of liquid metals.

1.1. Neutron scattering techniques

A neutron scattering experiment on an isotropic monatomic sample can measure the double differential scattering cross section:

$$\frac{d^2\sigma}{d\Omega\, d\omega} = \frac{k}{k_0}\left\{\frac{\sigma_{inc}}{4\pi}S_{inc}(Q,\omega) + \frac{\sigma_{coh}}{4\pi}S_{coh}(Q,\omega)\right\} \tag{1}$$

Here k_0, k are the incident and scattered wavevectors of the neutron and

$$\hbar Q = \hbar(k_0 - k) \qquad \hbar\omega = \frac{\hbar^2}{2m}(k_0^2 - k^2)$$

are the momentum and energy transfers in the scattering process.

If the sample is isotropic, the direction of Q is unimportant and Q can be replaced by its magnitude. S_{inc} and S_{coh} are the dynamic structure factors describing the effect of single-particle motion and the relative motion of two particles respectively on the scattering. The dynamic structure factors are Fourier transforms of the corresponding spacetime correlation functions of van Hove.

If σ_{coh} and σ_{inc} can be varied or if σ_{inc} is due to spin–flip scattering S_{inc} and S_{coh} can be separated. Information on single-particle dynamics can be extracted from S_{inc} and on collective dynamics from S_{coh}.

In practice the measured data must be corrected for background, sample environment, multiple scattering, instrument resolution etc before the true single-scattering data are available. This is now a well established procedure for which computer program packages exist.

2. Physics of diffusion processes

Incoherent quasi-elastic scattering is especially useful for studying single-particle diffusion. In the simple case of Brownian motion $S_{inc}(Q,\omega)$ takes the form

$$S_{inc}(Q,\omega) = \frac{1}{\pi}\frac{DQ^2}{(DQ^2)^2 + \omega^2} \tag{2}$$

which is more generally valid for Q extrapolated to zero.

The diffusion coefficient D can be determined by extrapolation:

$$D = \lim_{Q\to 0}\frac{1}{\pi Q^2 S_{inc}(Q,0)}. \tag{3}$$

As an example figure 1 shows data on liquid sodium at $T = 800$ K. The D values for liquid Na from neutron scattering are in quite good agreement with more recent results from the pulsed NMR technique [1] although the latter data are more restricted in their temperature range, and interpretation is less direct.

In principle with neutrons one could examine the diffusion process in more detail. And indeed it was shown by Morkel *et al* [2] in a careful analysis of the measured $S_{inc}(Q,\omega)$ of liquid Na at different temperatures that the basic mechanism of diffusion is more complex. $S_{inc}(Q,\omega)$ with increasing Q deviates from a Lorentzian. Figure 2 shows the halfwidth of the quasi-elastic S_{inc} of Na divided by DQ^2 at 800 K and a corresponding effect is seen in the reduced peak height. These data confirm similar deviations found in molecular dynamics simulations [3] and they could be explained by mode coupling theories [4].

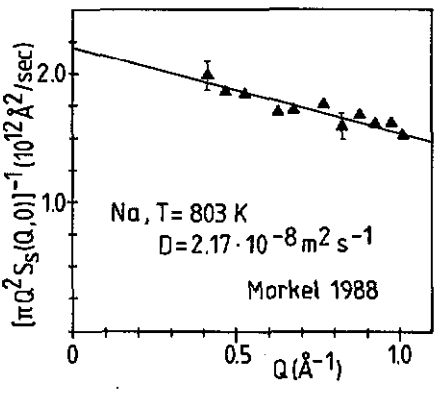

Figure 1. Determination of the diffusion coefficient D of liquid sodium at $T = 803$ K by the extrapolation procedure.

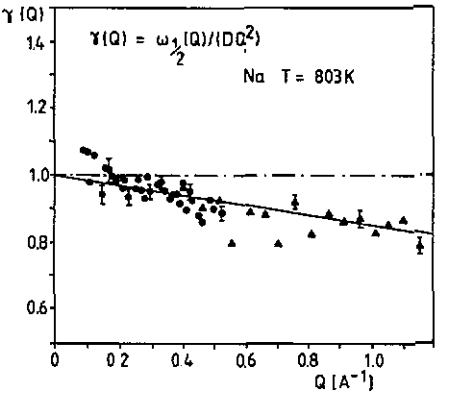

Figure 2. Reduced halfwidth $\gamma(Q)$ of $S_{\rm inc}(Q,\omega)$ of liquid sodium at 803 K.

The appropriate memory function for describing the effect is the velocity autocorrelation function of a moving particle in a liquid $z(\tau) = \langle v(0)v(\tau)\rangle$. For Brownian motion $z(\tau)$ decays exponentially. However, simulations and mode coupling calculations have already shown that, for hard sphere liquids, after an initial exponential decay, $z(\tau)$ decays more slowly, that is it decays according to a power law $z(\tau) \simeq \tau^{-3/2}$. The motion pattern is not chaotic but has a vortex structure. These vortices are microscopic shear excitations which have moderately long lifetimes and delay the decay of $z(\tau)$. For a $t^{-3/2}$ decay the excitation spectrum should not be a Lorentzian around $\omega = 0$ as predicted for Brownian motion, but it should have a square root cusp at $\omega = 0$, i.e. no horizontal but a vertical tangent.

The sodium data are in qualitative agreement with this picture as shown in figure 3. From the slope of $z(\omega)$ the shear viscosity follows in good agreement with values from the literature. These memory effects also probably play an important role in the microscopic behaviour of more complex liquids. They were found, for example, in liquid argon and dense H_2 [5] by Verkerk *et al.* This technique is now used when searching for deviations from the simple mode-coupling picture. An atom in a dense liquid does not perform Brownian motion—a free flight interrupted by stochastic collisions. It rattles in a cage formed by its neighbours' exciting shear vortices before it finds a way to change its position.

3. Collective atomic motions (inelastic neutron scattering)

Fortunately more data on coherent scattering samples are available. Coherent neutron scattering yields information on the relative arrangement and relative motion of atoms in a liquid. Without an energy analysis the static structure factor $S(Q)$ and hence the static pair distribution $g(r)$ is obtained from which, in principle, a pair potential can be extracted. An energy analysis supplies information on the collective motions.

In the generalized hydrodynamic theory of relaxation in liquids the dynamic structure factor $S(Q,\omega)$ can be written

$$S(Q,\omega) = \frac{k_{\rm B}TQ^2}{\pi M}\frac{{\rm Re}[M(Q,\omega)]}{|\omega_0^2 - {\rm i}\omega M(Q,\omega) - \omega^2|^2} \qquad \omega_0^2 = k_{\rm B}TQ^2/MS(Q). \tag{4}$$

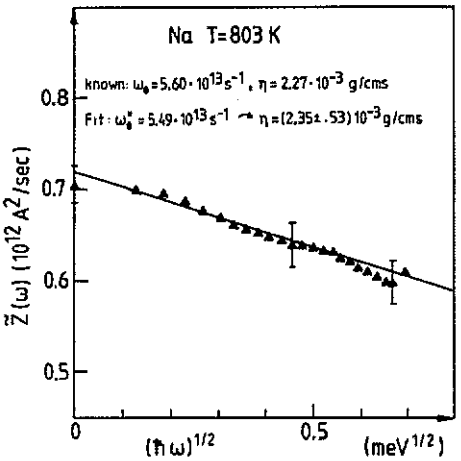

Figure 3. Frequency distribution $z(\omega)$ of liquid sodium at $T = 803$ K and small ω.

Here $M(Q,\omega)$ is a viscous damping function for excitations, or more formally the Laplace transform of the memory function for the longitudinal current–current correlation. $M(Q,\omega)$ is unknown and complex; however, in principle some information on $M(Q,\omega)$ should be directly extractable from the experimental data.

During the last 30 years many articles have been written, suggesting more or less simple approximations for $M(Q,\omega)$. (For example the visco-elastic model assuming an exponential decay of M governed by one relaxation time.)

On the other hand most of the neutron experiments have searched for propagating modes, essentially by trying to detect peaks in the $S(Q,\omega)$ spectrum. Copley and Lovesey achieved some encouraging results on liquid Rb [6]. These data have served as a test case for several molecular dynamics simulations [7].

An extensive analysis of the dynamics of liquid lead and bismuth was performed recently by Larsson *et al* [8] using neutron scattering and computer simulation data. The simulation data are in reasonable agreement with the experimental data for those Q-values where a comparison is possible. The authors concentrated on an analysis of the memory function which in the time domain showed a rapid decay at short times and a tail at longer times, suggesting at least the need for two relaxation times in models for the memory function as was recognized earlier by Levesque *et al* [9]. The Laplace transform at $\omega = 0$ can be interpreted as a generalized longitudinal viscosity

$$\gamma_1(Q) = M(Q,0)/Q^2 = \pi v_0^2 S(Q,0)/S(Q)^2 \tag{5}$$

which if temperature fluctuations can be neglected extrapolates to the well known hydrodynamic limit $\gamma_1(0,0) = \frac{4}{3}\gamma_s + \gamma_B$. The computer simulations made the transversal current correlation and therefore the generalized shear viscosity available. For increasing Q there is a tendency for the generalized longitudinal and shear viscosity to approach each other (in fact their ratio oscillates) whereas for $Q < Q_0$ (Q_0 is the position of the maximum of $S(Q)$) there is a marked difference. From this type of comparison it was concluded that for $Q > Q_0$ effects of self-motion are dominant and any collective activity may be only of short range in space and time.

There is some interesting structure in $\gamma_1(Q)$ in the vicinity of the maximum of the structure factor. Balucani *et al* [10] found an indication of a similar weak anomaly

in simulations of liquid rubidium. However, in experimental data on liquid caesium [11] nothing particular shows up in the vicinity of the position of the structure factor maximum.

3.1. Experimental results on liquid Cs

The experiments on liquid Cs were performed on three-axes spectrometers at ILL and FRM Munich. Q-ranging from 0.2 to 2.5 Å^{-1} was covered ($S(Q)_{max}$ at $Q_0 \simeq 1.4\ \text{Å}^{-1}$). The measured intensities were corrected in the usual way to obtain absolute $S(Q,\omega)$ data. Several of the resulting data sets are plotted in figure 4. The correction for the small incoherent scattering contribution leads to relative large errors at small Q and ω, but did not seriously affect the inelastic region.

The smooth curves are fits with a memory function ansatz with two relaxation times. The data are still sufficiently accurate to derive a number of microscopic quantities of the liquid. For example the longitudinal current correlation spectra are illustrated in figure 5. The peak positions of these spectra which correspond to the dispersion of the excitation spectra at small Q are plotted in figure 6.

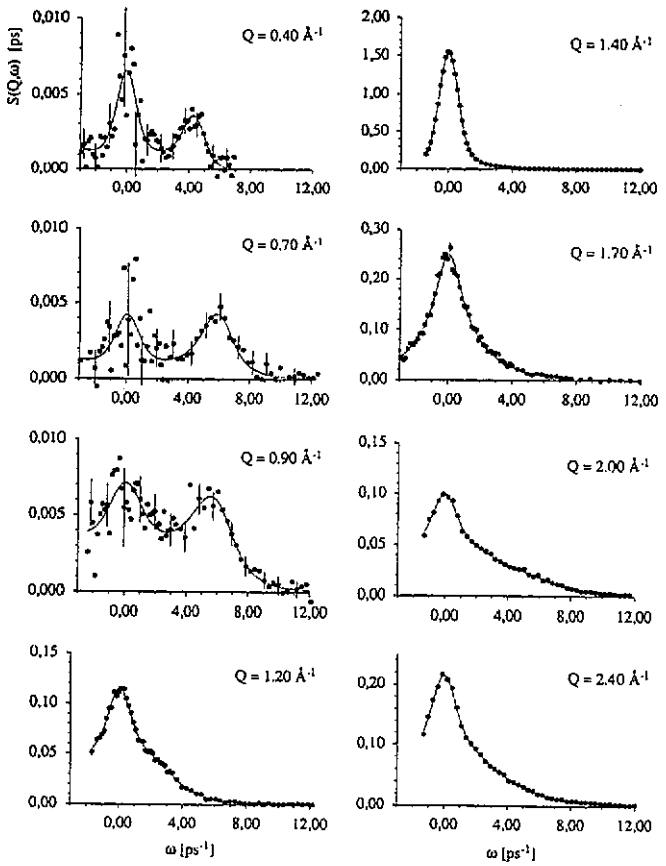

Figure 4. Dynamic structure factor $S(Q,\omega)$ of liquid caesium at $T = 308$ K: full dot, experimental data; broken line, parametrized form.

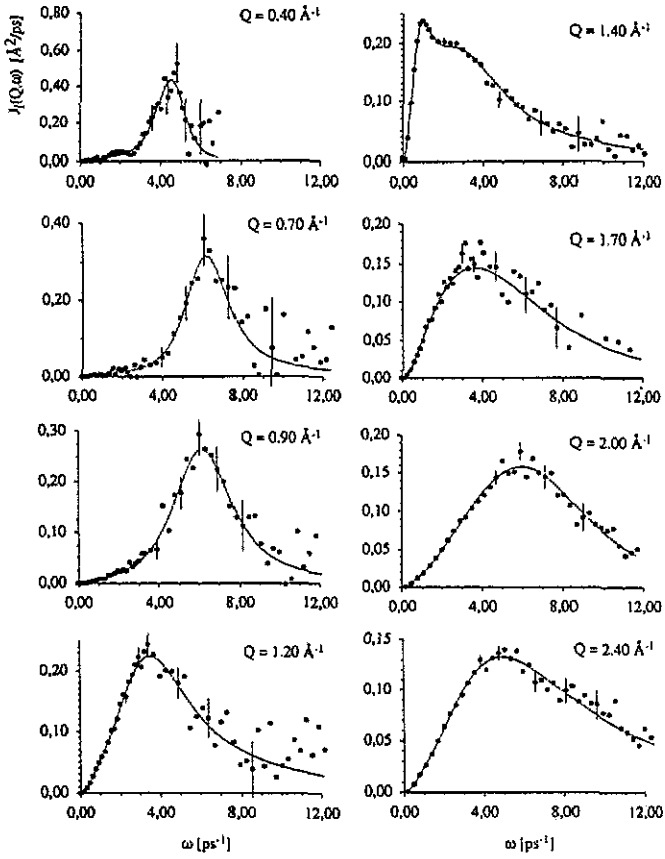

Figure 5. Longitudinal current correlation $J_1(Q,\omega)$ of liquid caesium at $T = 308$ K.

One can see a clear enhancement of the slope of this disperson compared with the acoustic sound velocity which is known for Cs at $T = 308$ K to be 965 m s^{-1} and should be the hydrodynamic limit of $\omega_m(Q)$. This enhancement is believed to be caused by the onset of shear relaxation at higher frequencies.

From the generalized hydrodynamic memory function

$$M(Q,\omega) = (\gamma - 1)\omega_0^2 \frac{\tau_H}{1 - i\omega\tau_H} + (\omega_1^2 - \gamma\omega_0^2)\frac{\tau_\eta}{1 - i\omega\tau_\eta} \tag{6}$$

where τ_H and τ_η are the relaxation times for heat diffusion and viscous damping, the disperson of propagating modes can be derived. As long as $\omega\tau_H \gg 1$ two limits for the disperson can be given [10]:

(i) $\omega\tau_\eta \ll 1 \Rightarrow \omega = c_s Q$ with $c_s = (\gamma k_B T/S(Q)M)^{1/2}$ the adiabatic sound velocity; and

(ii) $\omega\tau_\eta \gg 1 \Rightarrow \omega = c_\infty Q, c_\infty = \omega_1/Q$ where ω_1 is related to the fourth moment of $S(Q,\omega)$.

The values c_s and c_∞ are indicated in figure 7 for liquid Cs. The shear modulus and the Maxwell relaxation time can be determined from $C_\infty = \sqrt{3}G_\infty/\rho$ and $\tau_M = \eta_s/G_\infty$. A similar analysis has been performed for liquid Rb [12] leading to similar results.

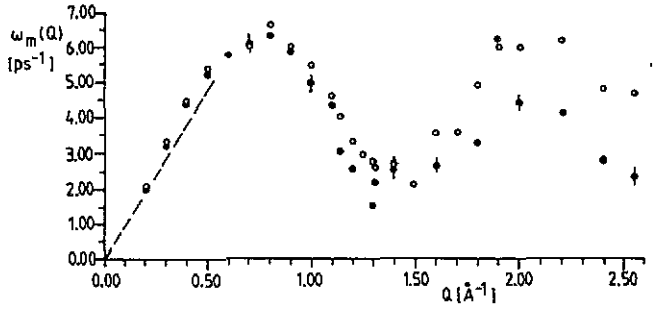

Figure 6. Disperson $\omega_m(Q)$ of the longitudinal current correlation $J_1(Q,\omega)$ (open circles and points are peak positions of $S(Q,\omega)$).

4. General memory function analysis

It was mentioned earlier that the memory function ansatz can be used to extract information on its Q- and ω-dependence from the experimental $S(Q,\omega)$ data. One can rewrite the general expression (4) for $S(Q,\omega)$ in the form of quadratic equations for the real and imaginary part of $M(Q,\omega)$ and solve the equations for some specific ω-values, given $S(Q,\omega)$ [13]. Alternatively one can take a model for $M(Q,t)$ containing two relaxation times which may extrapolate to the ones for heat diffusion and viscous damping in the hydrodynamic limit and then fit this model to the data.

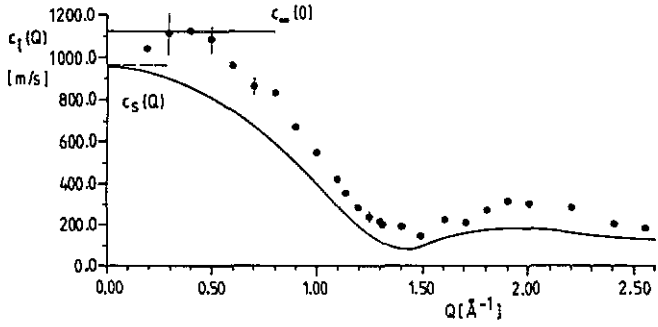

Figure 7. Positive dispersion and solid-like sound propagation in liquid caesium ($c_s = \sqrt{\gamma/S(Q)}v_0, c_\infty = \sqrt{3G_\infty/\rho}$).

Figure 8 illustrates the results from both techniques for the liquid Cs case. Fitting and direct evaluation are in reasonable agreement. These data also confirm that, in contrast to $S(Q,\omega)$, $M(Q,\omega)$ is a relatively smooth structureless function over most of the ω-range covered in the experiment, although there is a marked variation with Q. The two relaxation times are, however, quite different: at least one order of magnitude, as illustrated in figures 9(a) and (b). It is also interesting to look at the Q-dependent relative weight of these two contributions to the memory ansatz, shown in figure 9(c).

The domination of the short relaxation time around the position of $S(Q)_{max}$ is an indication that in this Q range essentially only one relaxation process survives and is therefore responsible for the decay of the density fluctuations. The structural relaxation is much slower than the decay of the fast density fluctuations.

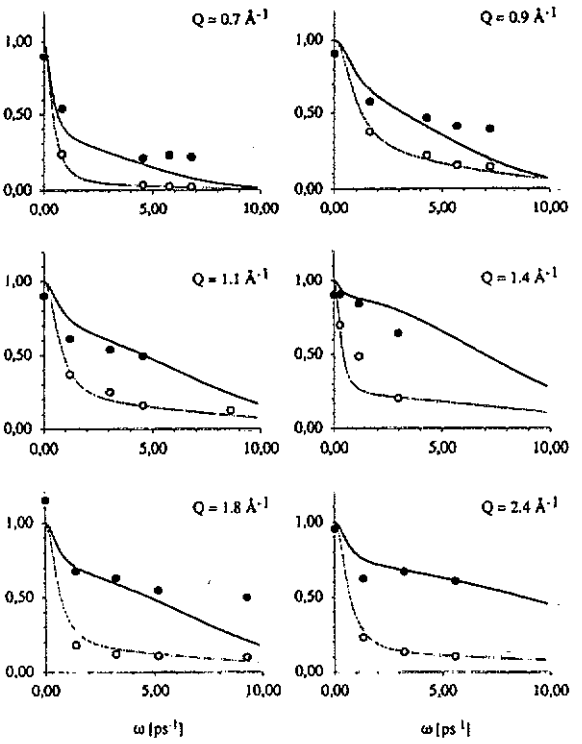

Figure 8. Relative values of real $M'(Q,\omega)$ (full curve) and imaginary part $M''(Q,\omega)$ (broken line) of $M(Q,\omega)$ from fitting (lines) and direct determination (points).

This is the reason why in a dense liquid in this region the contribution of relaxations other than structural relaxations can be neglected in the first order and the structural relaxation can be interpreted as a slow hydrodynamic-like diffusion process. A description of the central line as a diffusion-like decay process in the frame of the Enskog model [14] is illustrated in figure 10 giving an Enskog diffusion coefficient which compares favourably with the self-diffusion coefficient of liquid caesium.

This dominance of one relaxation time near $S(Q)_{\max}$ was recently confirmed by simulations for liquid rubidium where it was also found that the decay rate is slower than predicted by visco-elastic theories [15] due to mode coupling effects. With respect to the excitations, a model analysis has been performed, e.g. using the generalized eigenmode expansion following from the kinetic theory of hard sphere fluids [16] and the excitation spectrum of the density fluctuation can eventually be extracted for all Q. The model can be written

$$S(Q,\omega) = \frac{1}{\pi}\sum_{j=-\infty}^{+\infty} \mathrm{Re}\,\frac{A_j(Q)}{\mathrm{i}\omega + z_j(Q)} \qquad \sum_{j=-\infty}^{+\infty} A_j(Q)[z_j(Q)]^n = R_n(Q) \tag{7}$$

where $A_j(Q)$ and $z_j(Q)$ are the complex amplitudes and frequencies of the modes and the $R_n(Q)$ are the frequency moments of $S(Q,\omega)$. Although this is only an approximation, a three mode assumption may already give some valuable information. In the case of rare gas fluids for Q-values around Q_0 the sound mode eigenvalues turned out to be real leading to a sum of three Lorentzians about $\omega = 0$ or a gap in

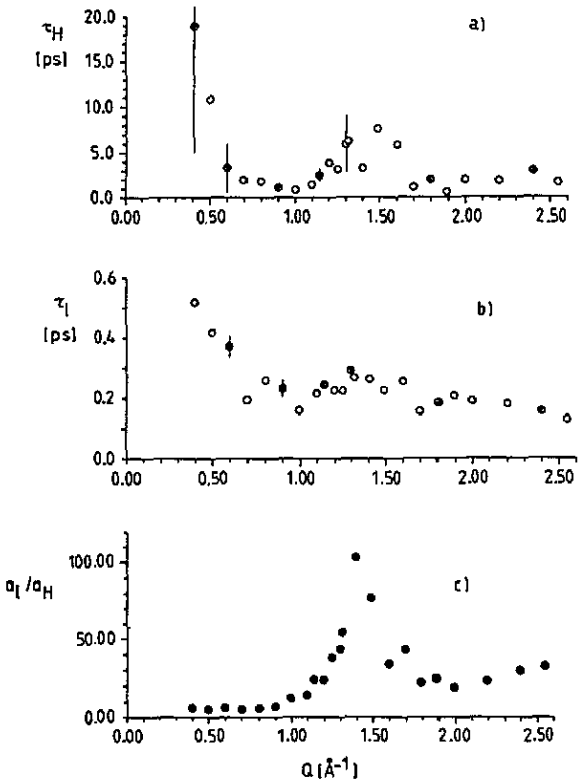

Figure 9. Relaxation times τ_H and τ_l as determined by the fitting procedure described in the text. (c) shows the relative weight of the two contributions.

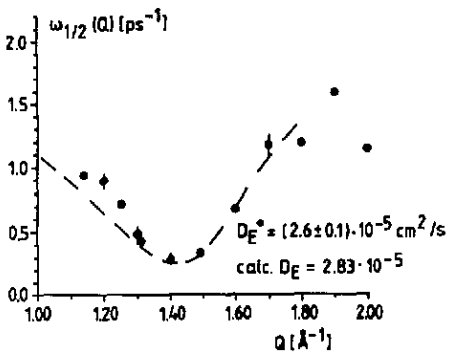

Figure 10. Halfwidth $\omega_{1/2}(Q)$ of the central part of $S(Q,\omega)$ of liquid caesium compared with the Enskog model.

the disperson as shown by de Schepper *et al* [16]. For liquid metals like caesium this does not seem to be the case as is illustrated in figure 11.

If we assume equality of the real and imaginary parts of the complex frequency as the limit for propagation, then the observed modes should be propagating ones even for Q-values beyond Q_0 the position of the maximum structure factor. They come close to the damping limit around Q_0 and are overdamped much further out. It is not

surprising that they cannot be seen as reasonable side peaks for $Q > 1.1$ Å^{-1} because for clear visibility ω_s/z_s should be greater than 4 [17].

The direct local memory function analysis leads to more accurate results. If we express the inverse of $M(Q,\omega)$ by a normalized function $\sigma = \sigma_1 + i\sigma_2$, then a quadratic equation for σ_1 and σ_2 can be derived [13]:

$$n\sigma_1 = (1-x^2)^2\sigma_1^2 + [\sigma_2(1-x^2) + cx]^2 \tag{8}$$

where $n = S(Q,0)/S(Q,\omega)$, $x = \omega/\omega_0$ and $c = \omega_0\pi S(Q,0)/S(Q)$. σ_1 and σ_2 therefore can be determined at several (6) x-values from the measured data. It turned out that for liquid caesium the σ_1 and $\sigma_2^0 = \sigma_2/\omega$ are only weakly ω-dependent for each Q. One can formulate a criterion for mode damping in terms of these functions and this is illustrated in figure 12. The hatched line marks the boundary $\omega_s = z_s$. The determined σ-pairs lie outside this damping region. The insert shows the ratio ω_s/z_s following from the analysis. According to this approach modes should propagate at all the Q-values covered in the experiment.

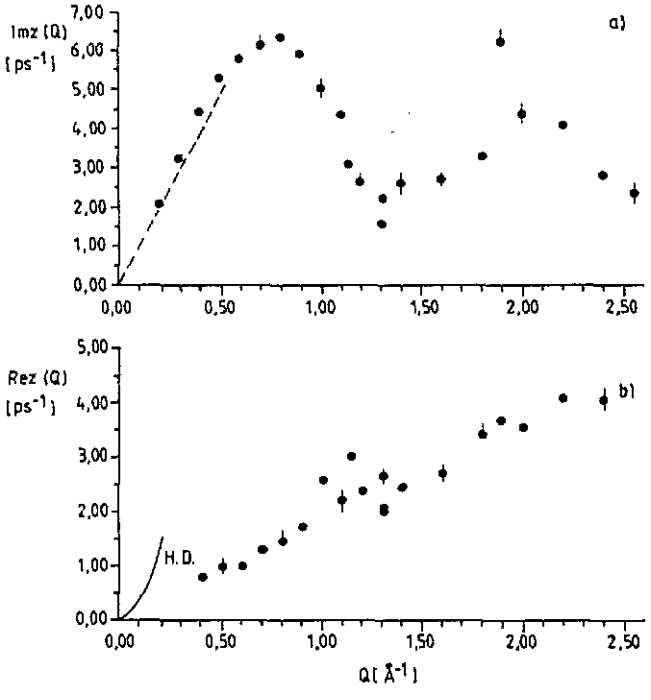

Figure 11. ω_s and $\omega_{1/2}$ from fitting the three-term approximation of the eigenmode expansion to the liquid caesium data.

One can compare the mode frequencies of this analysis with the eigenmodes of a rare gas liquid (with ω_0 as the proper frequency scale) as illustrated in figure 13. Whereas the rare gas data show a gap at Q_0 the liquid metal data show a peak which is an effect restricted in space and time and resembles the residue of an optic mode. It would be interesting to trace these dramatic differences back to the differences in the potentials of the two systems.

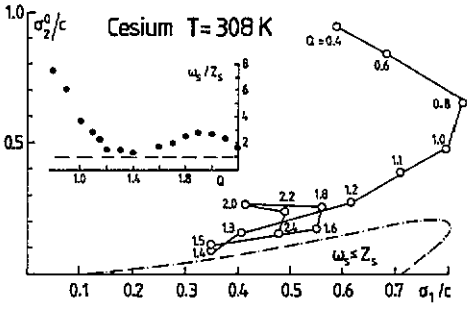

Figure 12. Relation between σ_2^0/c and σ_1/c for the liquid caesium data. The broken curve is the locus of points where $\omega_s = z_s$.

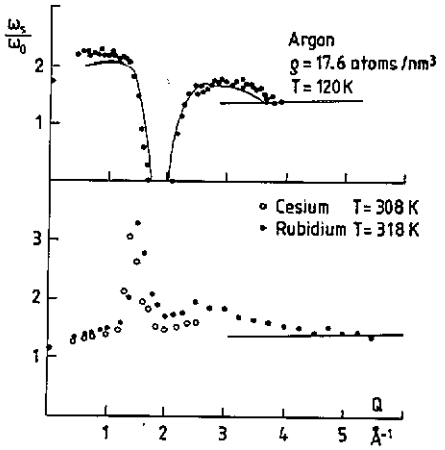

Figure 13. Comparison of the ratios ω_s/ω_0 for liquid argon with the values for liquid rubidium and caesium.

5. Conclusions

Improved neutron scattering techniques have made available more accurate data on simple monatomic liquids, like rare gas liquids and liquid metals. On the other hand with computer simulations the correlation functions of such systems which often cannot be measured can be calculated with computer simulations. The combined efforts are able to reveal details of single-particle motion which is more complex than Brownian diffusion and which can be explained by mode coupling theories. The same techniques applied to the study of collective atomic motions in liquids outside the hydrodynamic range have led to deeper insight into their properties. The study of the transition region now seems to be feasible.

A completion of this picture and a better quantitative understanding of the underlying damping mechanisms of motions still needs more effort as well as with computer simulations and theory.

References

[1] Pfiz T and Seeger A 1990 *Proc. 25th Congr. Ampère on Magnetic Resonance and Related Phenomena* (Berlin: Springer) p 494
[2] Morkel Chr, Gronemeyer Chr, Gläser W and Bosse J 1987 *Phys. Rev. Lett.* **58** 1873
[3] Alley W E and Alder B J 1983 *Phys. Rev.* A **27** 3158
[4] Bosse J, Götze W and Lücke M 1979 *Phys. Rev.* A **20** 1603
[5] Verkerk P, Builtjes J H and de Schepper I 1985 *Phys. Rev.* A **31** 1731
Montfrooy W and de Schepper I 1989 *Phys. Rev.* A **39** 2731
[6] Copley J D R and Lovesey S W 1975 *Rep. Prog. Phys.* **38** 451
[7] Rahman A 1974 *Phys. Rev.* A **9** 1667
[8] Larsson K-E, Gudowski W and Dzugutov M 1989 *Springer Proc. Phys.* **40** 13
[9] Levesque D, Verlet L and Kürkijarvi J 1973 *Phys. Rev.* A **7** 1690
[10] Balucani U, Vallauri R and Gaskell T 1987 *Phys. Rev.* A **35** 4263
[11] Bodensteiner T 1990 *PhD Thesis* TU München
[12] Morkel Chr and Bodensteiner T 1990 *J. Phys.: Condens. Matter* **2** SA251

[13] Egelstaff P A and Gläser W 1985 *Phys. Rev.* A **31** 3802
[14] de Schepper I M and Cohen E G D 1980 *Phys. Rev.* A **22** 287
[15] Balucani U and Vallauri R 1989 *Phys. Rev.* A **40** 2796
[16] de Schepper I M, van Rijs J C, van Well A A, Verkerk P and de Graaf L A 1984 *Phys. Rev.* A **29** 1602
[17] Gläser W and Egelstaff P A 1986 *Phys. Rev.* A **34** 2121